International Journal of Nanomedicine

Dovepress
Taylor & Francis Group

Open Access Full Text Article

ORIGINAL RESEARCH

Ampicillin-Loaded Fenugreek-Derived Exosomes Treat COPD via Anti-Inflammatory, Antibacterial and Anti-Fibrotic Effects

Haidiya Aierken[1], Bing Jia[1], Bahaerguli Aikeranmu[2], Pazula Aili[3], Weiming Yang[4], Changhao Zhong[5]

[1]Respiratory Center, The First Affiliated Hospital of Xinjiang Medical University, Urumqi, People's Republic of China; [2]Department of Respiratory Medicine, Bayingolin Mongolian Autonomous Prefecture People's Hospital, Urumqi, People's Republic of China; [3]Department of Clinical Medicine, Xinjiang Medical University, Urumqi, People's Republic of China; [4]School of Pharmacy, Kunming Medical University, Kunming, People's Republic of China; [5]State Key Laboratory of Respiratory Diseases, National Clinical Research Center for Respiratory Diseases, Guangzhou Institute of Respiratory Health, The First Affiliated Hospital of Guangzhou Medical University, Guangzhou, People's Republic of China

Correspondence: Changhao Zhong, Email Changhao_Zhong@outlook.com

Purpose: Chronic Obstructive Pulmonary Disease (COPD) is a major global health issue characterized by progressive airflow limitation, chronic inflammation, and recurrent infections. Current treatments largely alleviate symptoms but fail to simultaneously address infection-driven and inflammation-driven disease progression. Exosome-based strategies offer a promising alternative, and plant-derived exosomes possess distinct advantages, including low immunogenicity, natural abundance, and simple isolation compared with mammalian exosomes.

Methods: We developed a novel dual-functional nanotherapeutic agent by loading ampicillin into exosomes derived from *Trigonella foenum-graecum*. The resulting ampicillin-loaded exosomes (Exos-AM) harness the natural bioactivity and biocompatibility of plant exosomes to improve drug stability and cellular delivery. The therapeutic efficacy of Exos-AM was evaluated in a murine COPD model induced by lipopolysaccharide (LPS) instillation, cigarette smoke exposure, and *P. aeruginosa* infection.

Results: In vitro, Exos-AM exhibited potent antibacterial activity against *S. aureus, E. coli*, and *P. aeruginosa*, while promoting macrophage polarization toward the anti-inflammatory M2 phenotype, thereby alleviating inflammation and attenuating fibrotic responses. Transcriptomic analysis further revealed that Exos-AM modulated macrophage activation through suppression of the NF-κB and MAPK signaling pathways, providing mechanistic insight into its anti-inflammatory effects. In vivo, Exos-AM treatment significantly improved lung histopathology and enhanced bacterial clearance.

Conclusion: Our findings underscore the promise of plant-derived exosomes as versatile drug delivery platforms and position Exos-AM as a compelling therapeutic strategy for COPD by concurrently targeting infectious and inflammatory drivers.

Keywords: COPD, plant-derived exosomes, macrophage polarization, antibacterial, anti-fibrosis

Introduction

Chronic Obstructive Pulmonary Disease (COPD) stands as a formidable global health burden, currently ranked as the third leading cause of death worldwide.[1] It is characterized by persistent and often progressive airflow limitation associated with a chronic inflammatory response in the airways and lung parenchyma, primarily triggered by noxious particles or gases, most notably cigarette smoke.[2] The pathophysiology of COPD is complex and multifaceted, encompassing a destructive interplay between sustained inflammation, recurrent microbial infections, accelerated aging, and aberrant tissue repair processes.[3–6] Central to this pathology is the dysregulation of innate immune cells, particularly macrophages.[7,8] Upon chronic exposure to irritants, macrophages are predominantly polarized towards a pro-inflammatory M1 phenotype, releasing a cascade of inflammatory mediators such as TNF-α, IL-1β, and inducible nitric oxide synthase (iNOS).[9] This creates a perpetual inflammatory milieu that damages alveolar structures and promotes small airway fibrosis.[10] Conversely, the alternative anti-inflammatory M2 phenotype, characterized by markers like CD206 and Arg-1, which facilitates inflammation resolution and

https://doi.org/10.2147/IJN.S578352
Received: 17 November 2025
Accepted: 28 February 2026
Published: 19 March 2026

Graphical Abstract

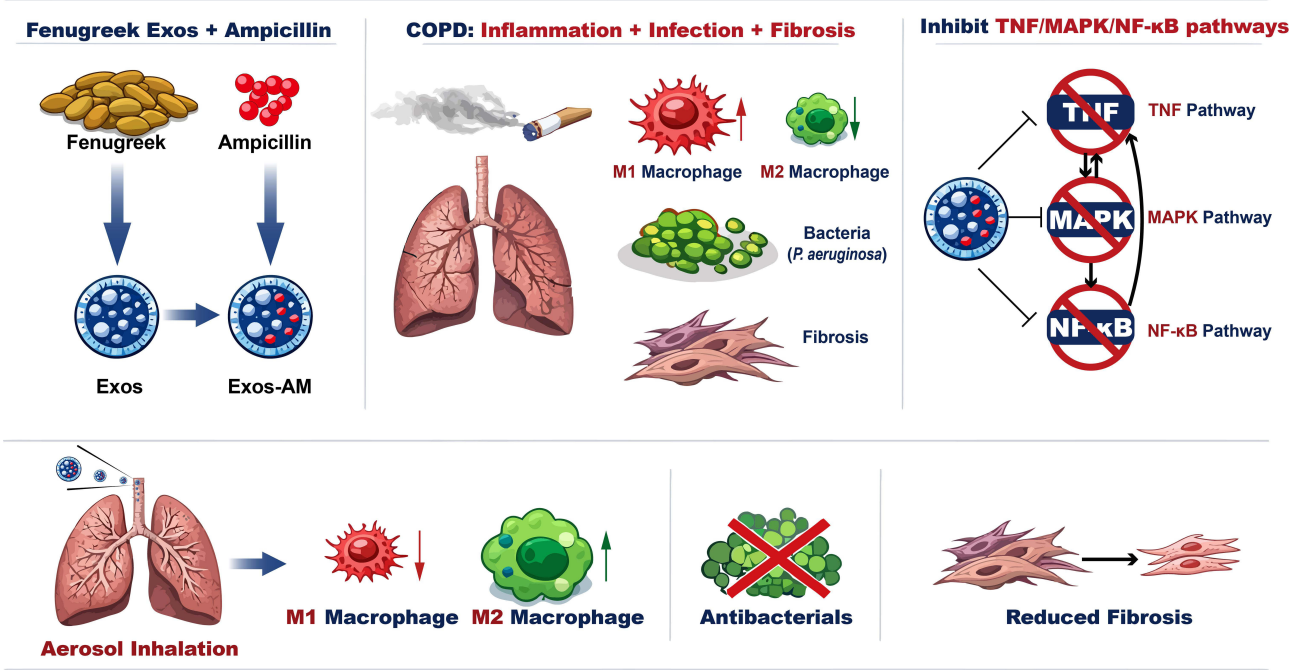

tissue repair, is often insufficient in COPD lungs.[11] Therefore, therapeutic strategies that can actively repolarize macrophages from the detrimental M1 state to the protective M2 state hold immense promise for halting disease progression.

Recent studies have revealed that macrophage polarization is not a simple M1/M2 dichotomy but a dynamic and metabolically regulated process shaped by cytokine signaling,[12] oxidative stress,[13] and microenvironmental cues.[14] Dysregulated signaling through pathways such as NF-κB drives persistent inflammatory activation of macrophages,[15] which is also a central mechanism contributing to chronic inflammation in COPD. Meanwhile, exosome-mediated molecular communication offers new opportunities to modulate macrophage activity and re-establish immune homeostasis.[16]

Compounding the chronic inflammation is the frequent colonization and infection of the COPD lung by bacterial pathogens, including *S. aureus, H. influenzae*, and *P. aeruginosa*.[17] These infections not only precipitate acute exacerbations, catastrophic events accelerating lung function decline and mortality, but also perpetuate chronic inflammation and contribute to the development of antibiotic resistance.[17–19] Thus, an ideal therapeutic regimen for COPD must incorporate potent antibacterial activity, capable of effectively clearing these persistent infections.

Pathological hallmark of advanced COPD is pulmonary fibrosis, particularly in the small airways.[20] Sustained inflammation and repetitive injury lead to the activation of lung fibroblasts and their differentiation into myofibroblasts, which excessively deposit extracellular matrix (ECM) proteins such as collagen I and III, driven by profibrotic factors like TGF-β.[21–23] This fibrotic remodeling narrows the airways and contributes irreversibly to airflow obstruction. Consequently, an effective anti-fibrotic capability is a vital component of a comprehensive COPD therapy.

Despite decades of research, current pharmacological management for COPD, primarily based on bronchodilators and corticosteroids, remains largely palliative.[24,25] These conventional treatments alleviate symptoms but fail to address the interconnected triad of inflammation, infection, and fibrosis that drives disease progression. Antibiotics alone are insufficient to regulate chronic inflammation, and anti-inflammatory agents have limited capacity to eliminate persistent pathogens. Therefore, there is an urgent need for novel strategies capable of simultaneously modulating inflammatory and infectious components while preventing tissue remodeling.

Exosomes, nano-sized extracellular vesicles derived from cell membranes, have gained considerable attention as promising therapeutic carriers due to their ability to deliver bioactive molecules to recipient cells.[26,27] As key mediators of intercellular communication, exosomes modulate immune responses, promote tissue repair, and suppress inflammation.[28–30] Recent evidence suggests that plant-derived exosomes represent a valuable therapeutic resource.[31–33] Compared to mammalian exosomes, they offer advantages such as low immunogenicity and easier isolation, making them attractive for clinical translation.[34] Exosomes from *Trigonella foenum-graecum*, a plant renowned in traditional medicine for its anti-inflammatory and health-restoring effects, represent a particularly promising yet underexplored biomaterial. Their natural composition suggests inherent biocompatibility and potential for enhanced uptake by immune cells like macrophages, making them an ideal smart delivery vehicle for pulmonary therapeutics.[35,36] In addition, inhalable exosome formulations have emerged as an effective delivery strategy for targeting lung tissues, providing improved bioavailability and local retention.[37,38]

Building on these insights, the present study differs from existing COPD treatment research by introducing a dual-target exosome-based platform that integrates antimicrobial and immunomodulatory functions within a single plant-derived carrier. In this study, we engineered a novel nanotherapeutic agent by loading the broad-spectrum antibiotic ampicillin[39] into fenugreek-derived exosomes (Exos-AM). This bio-hybrid system was designed to synergistically combine the intrinsic bioactivities of the plant exosomes with the targeted action of the antibiotic. Our work aimed to comprehensively evaluate the multifaceted functions of Exos-AM, including: (1) its enhanced antibacterial efficacy against common COPD pathogens via improved drug delivery and biofilm disruption; (2) its capacity to repolarize macrophages from the pro-inflammatory M1 phenotype toward the anti-inflammatory and tissue-reparative M2 phenotype, thereby mitigating chronic inflammation; and (3) its ability to suppress TGF-β1-induced fibroblast activation and migration, conferring a potent anti-fibrotic effect. We systematically investigated these functions through a series of in vitro assays and further validated the therapeutic potential of Exos-AM in a murine model of COPD induced by LPS and cigarette smoke exposure coupled with bacterial challenge (Figure 1). This work establishes plant-derived exosomes as a versatile and powerful platform for drug delivery and presents Exos-AM as a compelling, multi-targeted therapeutic strategy to address the complex pathology of COPD.

Materials and Methods

Preparation of Fenugreek Exosomes (Exos) and Ampicillin-Loaded Exosomes (Exos-AM)

Seeds of *Trigonella foenum-graecum* (commercially purchased from a market of Zigong city, Sichuan province, China) were cleaned, dried, and ground into powder. The powder was suspended in sterile PBS and subjected to ultrasonication (200 W, 20 kHz, 20 min) followed by differential centrifugation to remove debris (300×g, 2,000×g, and 10,000×g). The supernatant was ultracentrifuged at 100,000×g for 70 min at 4°C to collect exosomes (Exos).

To prepare Ampicillin-loaded Exos (Exos-AM), purified Exos were incubated with ampicillin (1mg/mL) under ultrasonication (100W, 5min) and then ultracentrifuged again to remove free drug. The final pellet was resuspended in PBS and stored at −80°C until use.

Characterization of Exos and Exos-AM

The morphology of Exos and Exos-AM was analyzed by scanning electron microscopy (SEM, Hitachi S-4800). Size distribution and zeta potential were determined using a Nano ZS Zetasizer (Malvern Instruments, UK). All measurements were repeated in triplicate.

Cell Culture

RAW264.7 murine macrophages and L929 mouse fibroblasts were obtained from the Chinese Academy of Sciences Cell Bank. RAW264.7 cells were cultured in DMEM supplemented with 10% fetal bovine serum (FBS), 1% penicillin–streptomycin at 37°C, 5% CO_2. L929 cells were maintained under the same conditions.

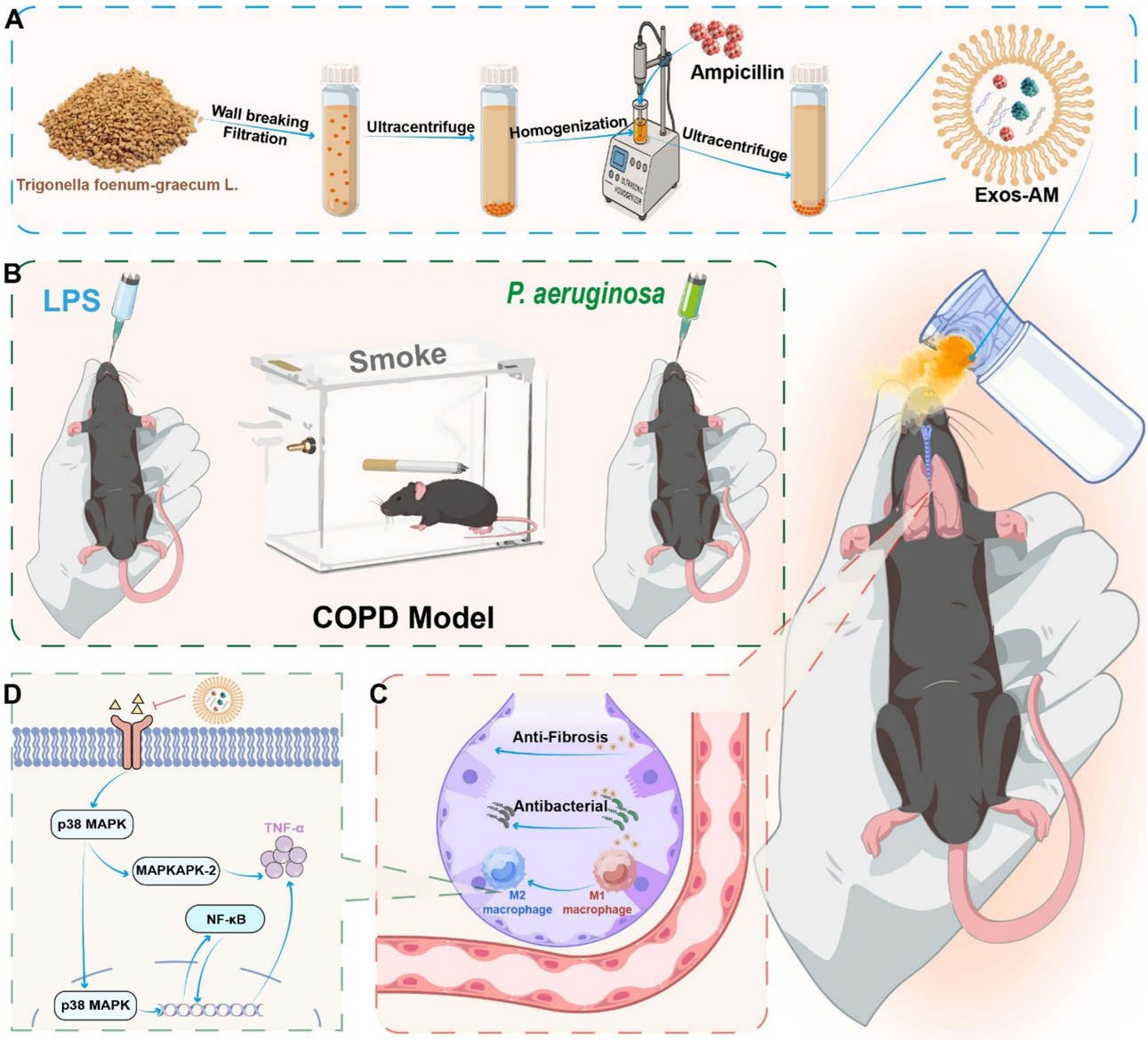

Figure 1 Application of Exos-AM in a COPD model. (**A**) Preparation of Exos-AM. (**B**) Establishment of the COPD model. (**C**) Biological effects of Exos-AM. (**D**) Molecular mechanisms of Exos-AM in a COPD model.

Biosafety of Exos and Exos-AM

Cell viability was assessed using the CCK-8 assay (Dojindo, Japan). Cells were seeded in 96-well plates and treated with various concentrations of Exos or Exos-AM (0–200 μg/mL) for 24 h. Absorbance was measured at 450 nm. LIVE/DEAD staining was performed using Calcein-AM and PI double-staining kits to visualize live and dead cells under fluorescence microscopy (Leica DMi8, Germany).

Antioxidant and Enzyme-Like Activity of Exos-AM

The radical scavenging abilities of Exos-AM were evaluated using $ABTS^{\cdot+}$, $DPPH^{\cdot}$, $PTIO^{\cdot}$, and TMB (3,3′,5,5′-Tetramethylbenzidine) assays following standard protocols. To further assess the intracellular ROS-scavenging capability, oxidative stress was induced in RAW264.7 macrophages and L929 fibroblasts using hydrogen peroxide (H_2O_2, 200 μM) for 2 h. After induction, cells were treated with Exos or Exos-AM (100 μg/mL) for 12 h. The intracellular ROS

 https://doi.org/10.2147/IJN.S578352

levels were measured using the DCFH-DA fluorescent probe (10 μM, 30 min incubation at 37°C). Fluorescence signals were observed and recorded under a fluorescence microscope (Leica DMi8, Germany).

Antibacterial Properties

The antibacterial effects of Exos and Exos-AM were tested against *Staphylococcus aureus* (*S. aureus*) (ATCC23235, USA), *Escherichia coli* (*E. coli*) (ATCC25922, USA), and *Pseudomonas aeruginosa* (*P. aeruginosa*) (ATCC27853, USA). Bacterial suspensions were adjusted to approximately 1×10^6 CFU/mL and incubated with PBS, Exos or Exos-AM (100 μg/mL) at 37 °C for 24 h. After incubation, aliquots were serially diluted and plated on LB agar for colony counting to determine bacterial survival rates. Biofilm formation was assessed using 0.1% (w/v) crystal violet staining after 24 h of incubation.

Macrophage Repolarization Assay

RAW264.7 cells were treated with LPS (100 ng/mL) and Exos or Exos-AM (100 μg/mL) for 24 h. Immunofluorescence staining was performed to detect iNOS and CD206 expression. Flow cytometry analysis was performed to quantify the expression of surface markers F4/80, CD86 (M1) and CD206 (M2). Western blotting was used to analyze the protein levels of iNOS, IL-1β, CD206 and Arg-1.

Fibrosis Inhibition in L929 Cells

Transwell migration and scratch wound healing assays were performed to evaluate L929 fibroblast mobility under TGF-β1 stimulation (5 ng/mL), with or without Exos-AM treatment. Cell migration was observed at 24 h. For the scratch wound healing assay, images were captured at 0 h and 24 h. The expression levels of fibrosis-related genes, including *α-sma, Col1a1, Col3a1*, and *Ctgf*, were quantified by real-time quantitative PCR (RT-qPCR) using GAPDH as the internal control.

RNA Transcriptome Sequencing

RAW264.7 cells were divided into LPS-treated and LPS + Exos-AM groups. Total RNA was extracted using TRIzol and sequenced using the Illumina platform. Differential gene expression analysis was performed using DESeq2. Enrichment analyses including GO and KEGG pathways were conducted to identify relevant biological processes.

In vivo COPD Model and Treatment

Female C57BL/6 mice (6–8 weeks, n = 6) were used to establish a COPD model through intranasal LPS (50 μg) on day −1, followed by daily cigarette smoke exposure for 3 weeks.[40] *P. aeruginosa* (10^6 CFU) was intranasally administered on week 3. Mice were treated with aerosolized Exos or Exos-AM (200 μg/mL, 20 min/day) for 5 days. On completion of the study, Mice were euthanized by exposure to a rising concentration of carbon dioxide (CO_2) at a flow rate displacing 30–70% of the chamber volume per minute, followed by a 4-minute exposure after respiratory arrest. Death was confirmed by cervical dislocation, in accordance with the AVMA Guidelines for Euthanasia of Animals. Lung tissues were collected for H&E staining, immunofluorescence (F4/80, iNOS, CD206), and bacterial quantification by plate culture.

In vivo Biosafety Evaluation

To assess biocompatibility, healthy mice were treated with aerosolized Exos or Exos-AM daily for 5 days. Major organs (heart, liver, spleen, lung, kidney) were harvested and subjected to H&E staining to evaluate histological changes.

Statistical Analysis

All experiments were performed in triplicate unless otherwise stated. Data are presented as mean ± standard deviation (SD). One-way ANOVA or Student's *t*-test was used for statistical comparisons using GraphPad Prism 9.0. Differences were considered statistically significant at $p < 0.05$.

Results and Discussion

Preparation and Characterization of Exos and Exos-AM

The exosomes (Exos) were successfully isolated from *Trigonella foenum-graecum* seeds using ultracentrifugation (Figure 2A). The morphology of the Exos and Exos-AM was observed by scanning electron microscopy (SEM), which revealed spherical, uniform particles (Figure 2B). TEM images of Exos-AM (Supplementary Figure S1) revealed a typical cup-shaped vesicular morphology consistent with the characteristics of exosomes. The DLS profiles (Figure 2C) showed a single peak distribution, with mean diameters of approximately 79 nm for Exos and 91 nm for Exos-AM, confirming the uniformity of the exosome population, which is crucial for their consistent behavior in both in vitro and in vivo experiments. This size is typical for exosomes and suggests that they are within the optimal range for cellular uptake and therapeutic applications.[41,42] The zeta potential measurements (Figure 2D) showed negative surface charges of about –6.7 mV for Exos and –6.9 mV for Exos-AM, reflecting good stability and resistance to aggregation, which are essential for prolonged circulation and efficient delivery in vivo.[43]

In terms of cellular biocompatibility, RAW264.7 macrophages and L929 fibroblasts were treated with various concentrations (0–200 μg/mL) of Exos and Exos-AM for 24 hours. The cell viability assays demonstrated that both Exos and Exos-AM did not induce significant cytotoxicity at 0–100 μg/mL, with cell viability remaining over 90% (Figure 2E). These results suggest that both Exos and Exos-AM at a concentration of 100 μg/mL are biocompatible, making them suitable for further in vitro applications. In addition, Live/Dead staining confirmed the viability of cells treated with 100 μg/mL Exos and Exos-AM, with most cells showing green fluorescence (indicating live cells) and extremely low red fluorescence (indicating dead cells) (Figure 2F and G).

Further investigation into the in vivo safety of Exos-AM was performed by examining major organs (heart, lung, liver, spleen, and kidney) from mice treated with Exos-AM. Histological analysis using H&E staining revealed no pathological changes or signs of inflammation in any of the organs (Figure 2H), suggesting that Exos-AM is safe for use in vivo and does not induce adverse effects. This is consistent with previous reports, which indicates that exosome-based formulations typically exhibit favorable biosafety profiles due to their natural composition.[44,45]

Antioxidant and Enzyme-Like Activities

The antioxidant potential of Exos-AM was systematically evaluated through a series of free radical scavenging assays, including DPPH·, $ABTS^{\cdot+}$, PTIO·, and hydroxyl radical (·OH) assays. As shown in Figure 3A–D, Exos-AM exhibited strong, concentration-dependent scavenging abilities against multiple radical species. The absorbance intensity of each radical solution gradually decreased with increasing Exos-AM concentration (0–100 μg/mL), indicating efficient neutralization of free radicals. Quantitative analysis further confirmed that the inhibition rates of DPPH·, $ABTS^{\cdot+}$, PTIO·, and ·OH radicals progressively increased and reached over 80% at 100 μg/mL (Figure 3E–I). These findings demonstrate that Exos-AM possesses potent antioxidant capacity, capable of effectively quenching diverse reactive oxygen species.

The notable radical-scavenging behavior of Exos-AM can be attributed to the natural bioactive constituents derived from fenugreek exosomes, which are rich in phenolic and flavonoid compounds with intrinsic redox activity.[46] In addition, Exos-AM exhibited superoxide dismutase (SOD)-like activity, suggesting that it can mimic enzymatic antioxidant functions to convert superoxide radicals into less reactive oxygen species, providing an enzyme-like catalytic defense mechanism.[47,48]

To further validate the intracellular antioxidant effects, oxidative stress was induced in L929 fibroblasts and RAW264.7 macrophages using H_2O_2. As shown in Figure 3J, cells exposed to H_2O_2 alone displayed strong green fluorescence due to excessive intracellular ROS accumulation, whereas treatment with Exos and Exos-AM significantly reduced fluorescence intensity, indicating efficient ROS scavenging within cells. This result confirms that Exos and Exos-AM not only eliminates extracellular radicals but also alleviates oxidative stress at the cellular level. This result is similar to the Sowmya's report.[49]

The Live/Dead staining results (Figure 3K) further corroborated these findings. Cells challenged with H_2O_2 exhibited extensive red fluorescence (dead cells), while those treated with Exos and Exos-AM maintained predominant green

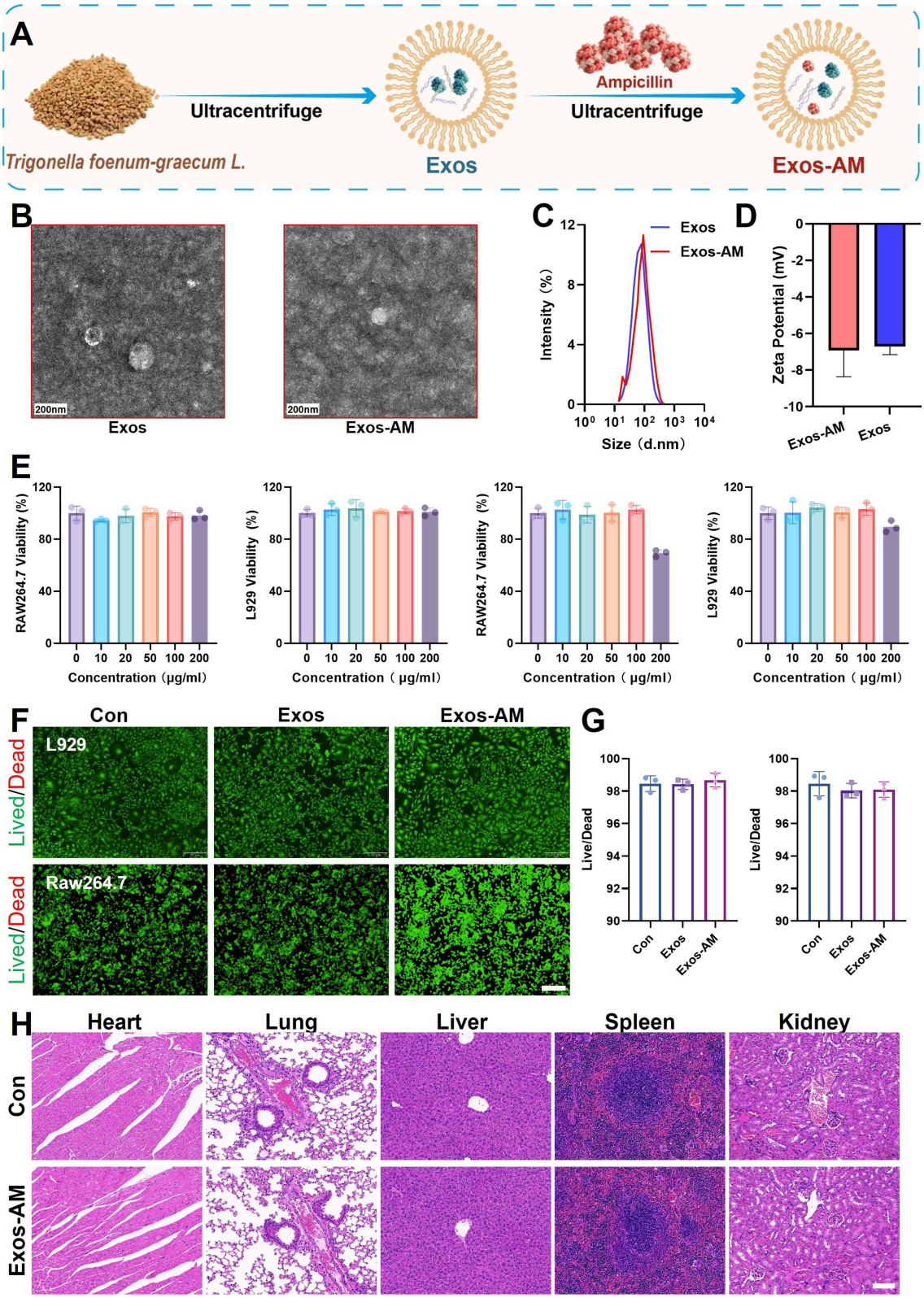

Figure 2 Preparation and Characterization of Exos and Exos-AM. (**A**) Schematic representation of the preparation process for Exos and Exos-AM. (**B**) SEM images of Exos and Exos-AM. (**C**) Particle size distribution of Exos and Exos-AM. (**D**) Zeta potential analysis of Exos and Exos-AM. (**E**) Cell viability of RAW264.7 and L929 cells. (**F**) Live/Dead staining of L929 and RAW264.7 cells. Bar = 100μm. (**G**) Quantification of cell viability via Live/Dead staining. (**H**) H&E staining of heart, lung, liver, spleen and kidney from mice treated with Exos-AM. Bar = 100μm. Data are presented as mean ± SD.

https://doi.org/10.2147/IJN.S578352

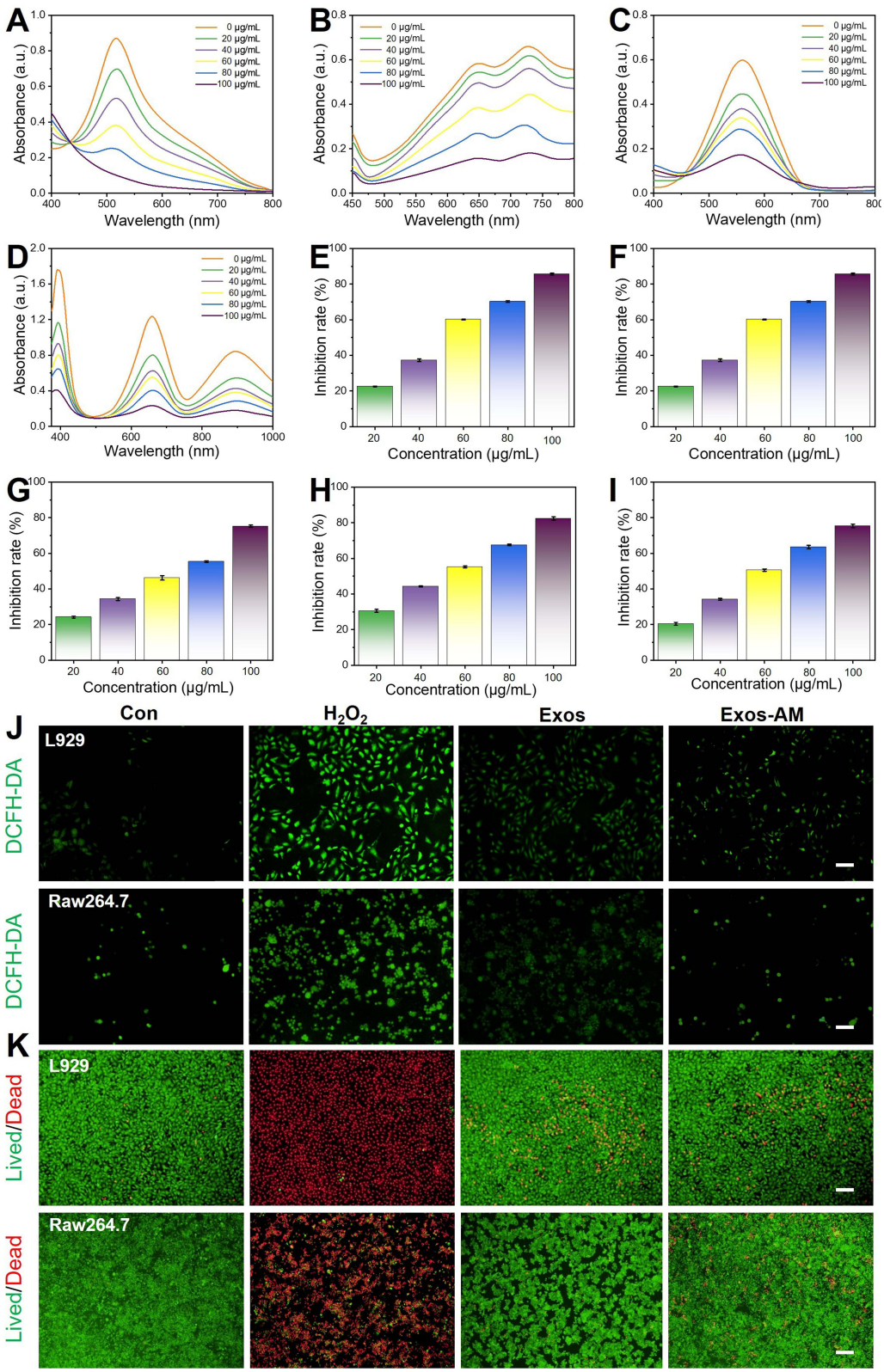

Figure 3 Antioxidant and Enzyme-Like Activities. (**A** and **E**) DPPH · scavenging and clearance ratio. (**B** and **F**) ABTS · scavenging and clearance ratio. (**C** and **G**) PTIO · scavenging and clearance ratio. (**D** and **H**) ·OH- scavenging and clearance ratio. (**I**) SOD-like enzyme activity and ·O2- scavenging ratio. (**J**) ROS staining of RAW264.7 cells. Bar = 100μm. (**K**) Live/Dead staining of RAW264.7 cells. Bar = 250μm. Data are presented as mean ± SD.

https://doi.org/10.2147/IJN.S578352

fluorescence, suggesting high cell viability and strong cytoprotective effects under oxidative stress. These data collectively indicate that Exos and Exos-AM effectively restores redox homeostasis and prevents oxidative damage in both macrophages and fibroblasts.

Antibacterial Efficacy of Exos and Exos-AM

To evaluate the antibacterial potential of Exos and Exos-AM, three representative bacterial strains—*S. aureus, E. coli, and P. aeruginosa*—were employed. As illustrated in Figure 4A, Exos and Exos-AM were co-incubated with bacterial suspensions for 24 hours, followed by bacterial plating and biofilm staining.

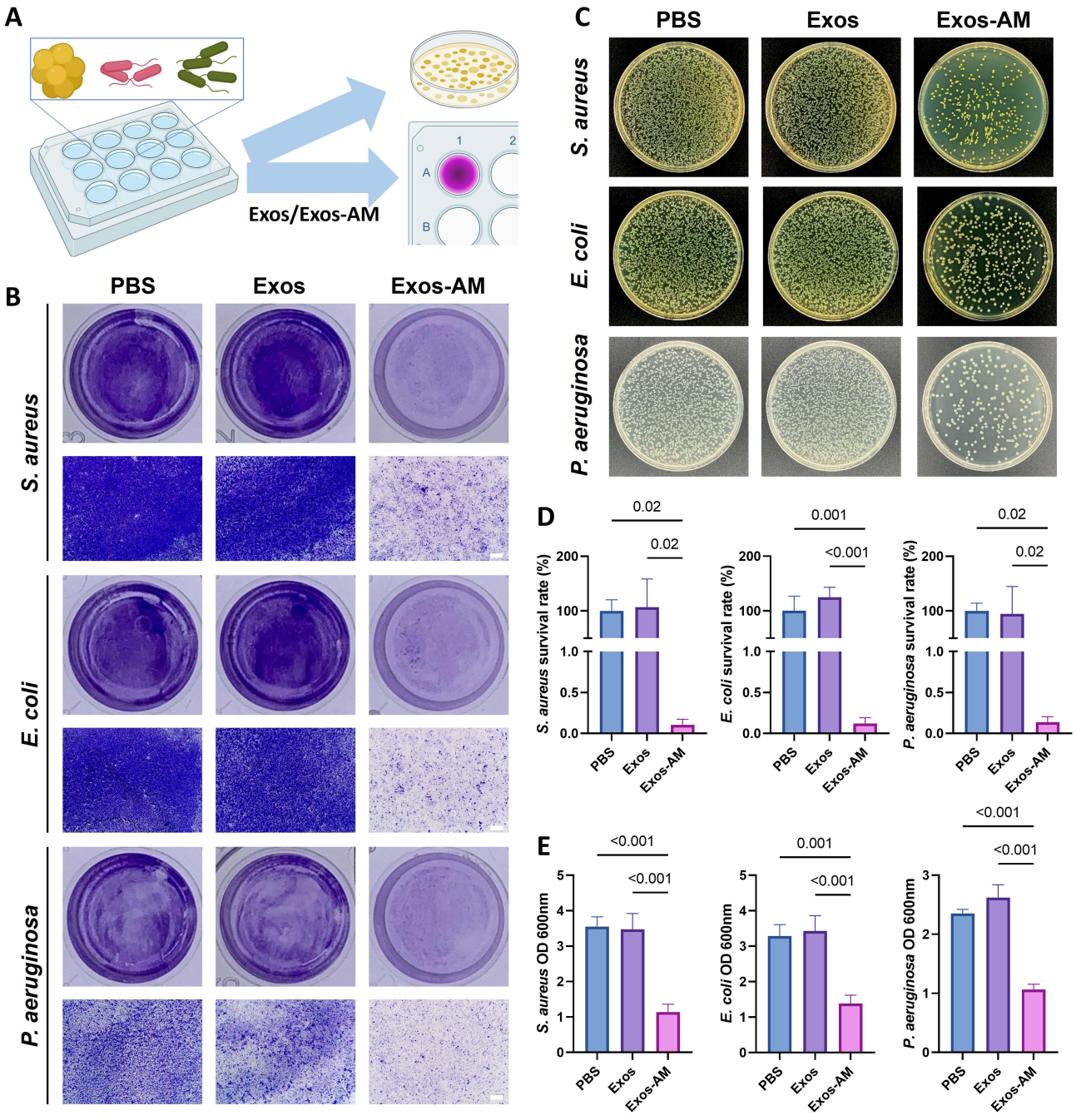

Figure 4 Antibacterial Efficacy of Exos and Exos-AM. (**A**) Schematic diagram of antibacterial experiment. (**B**) Crystal violet staining. Bar = 100μm (**C**) Plate coating results. (**D**) Bacterial survival based on plate coating results. (**E**) Bacterial OD 600nm measurements base on crystal violet staining. Data are presented as mean ± SD.

https://doi.org/10.2147/IJN.S578352

Crystal violet staining (Figure 4B) revealed that Exos-AM markedly inhibited bacterial biofilm formation compared with the PBS and Exos groups. The Exos-treated samples showed only slight attenuation of biofilm density, while Exos-AM treatment resulted in nearly transparent wells with minimal crystal violet retention, suggesting effective prevention of bacterial adhesion and biofilm development.

The colony-forming unit (CFU) assay results (Figure 4C) further confirmed the potent antibacterial activity of Exos-AM. Compared with PBS and Exos, Exos-AM significantly reduced bacterial colony numbers for all three strains. Quantitative analysis (Figure 4D) showed that the survival rates of *S. aureus, E. coli*, and *P. aeruginosa* after Exos-AM treatment dropped to 0.5%. In contrast, Exos alone only slightly decreased bacterial survival compared with the PBS control, indicating that the primary antibacterial effect originates from the ampicillin cargo rather than the exosomal membrane itself. The study of Yang et al also confirmed that the antibacterial function of antibiotic-loaded exosomes is achieved by antibiotics, not exosomes.[50] But there are also some special exosomes that can kill bacteria through beta-glycosidase, bacteriolytic enzymes.[51,52]

Similarly, biofilm biomass quantification (Figure 4E) demonstrated a remarkable reduction in OD_{600} for Exos-AM–treated groups across all bacterial species, confirming their strong inhibitory effect on biofilm formation. *S. aureus* and *E. coli* biofilms were especially sensitive to Exos-AM treatment, consistent with the expected susceptibility of Gram-positive and Gram-negative bacteria to β-lactam antibiotics.[53]

Similar trends have been reported in other exosome-based antimicrobial approaches. For instance, bacterial outer-membrane vesicles and mammalian exosomes have been used to deliver antibiotics or antimicrobial peptides, enhancing drug stability and targeted delivery.[54,55] However, these studies also indicated that exosome encapsulation primarily improves pharmacokinetics rather than altering host immune modulation, consistent with our findings for Exos-AM.

Compared to free amoxicillin reported in previous studies, the advantage of Exos-AM is encapsulation of Exos-AM, which facilitates better bacterial membrane penetration and local drug accumulation.[56] Moreover, the natural lipid composition of plant-derived exosomes might assist in disrupting bacterial cell envelopes, thereby potentiating antibiotic efficacy.[57]

Exos and Exos-AM Promote M2 Polarization of RAW264.7 Macrophages

To investigate the immunomodulatory effects of Exos and Exos-AM on macrophage polarization, RAW264.7 cells were first stimulated with LPS to induce a pro-inflammatory M1 phenotype, followed by treatment with Exos or Exos-AM. Immunofluorescence staining (Figure 5A–C) showed that LPS treatment significantly upregulated the M1 marker iNOS, as evidenced by strong red fluorescence, whereas both Exos and Exos-AM treatments reduced iNOS expression and enhanced the expression of the M2 marker CD206 (green fluorescence), suggesting a shift from the M1 to the M2 phenotype. However, no significant differences were observed between the Exos and Exos-AM groups, indicating that both treatments similarly promote M2 polarization and counteract the pro-inflammatory effects of LPS.

Flow cytometry analysis further confirmed this trend (Figure 5D–F). The percentage of $F4/80^{+}CD86^{+}$ M1 macrophages was significantly decreased in both the Exos and Exos-AM treatment groups, while the proportion of $F4/80^{+}CD206^{+}$ M2 macrophages increased comparably in both groups. These data suggest that Exos and Exos-AM exert similar immunoregulatory effects by promoting the differentiation of macrophages towards the M2 anti-inflammatory phenotype.

Western blot analysis (Figure 5G and H) showed consistent results, with both Exos and Exos-AM treatments leading to a significant downregulation of pro-inflammatory markers iNOS and IL-1β, alongside a substantial upregulation of M2-associated markers CD206 and Arg-1. These findings further demonstrate that Exos and Exos-AM similarly modulate macrophage polarization, shifting them towards an anti-inflammatory state without significant differences in their overall immunomodulatory capacity (Figure 5I).

The similar effects observed in both Exos and Exos-AM can be attributed to the bioactive molecules present in the exosomes themselves, which likely include proteins, lipids, nucleic acids and small molecules that are capable of modulating macrophage behavior.[58,59] Interestingly, the comparable immunoregulatory effects observed between Exos and Exos-AM suggest that the exosome carrier itself plays a crucial role in driving these effects. Plant-derived exosomes, especially those from Trigonella foenum-graecum, are known to contain bioactive lipids, proteins, and small RNAs that modulate inflammatory signaling and

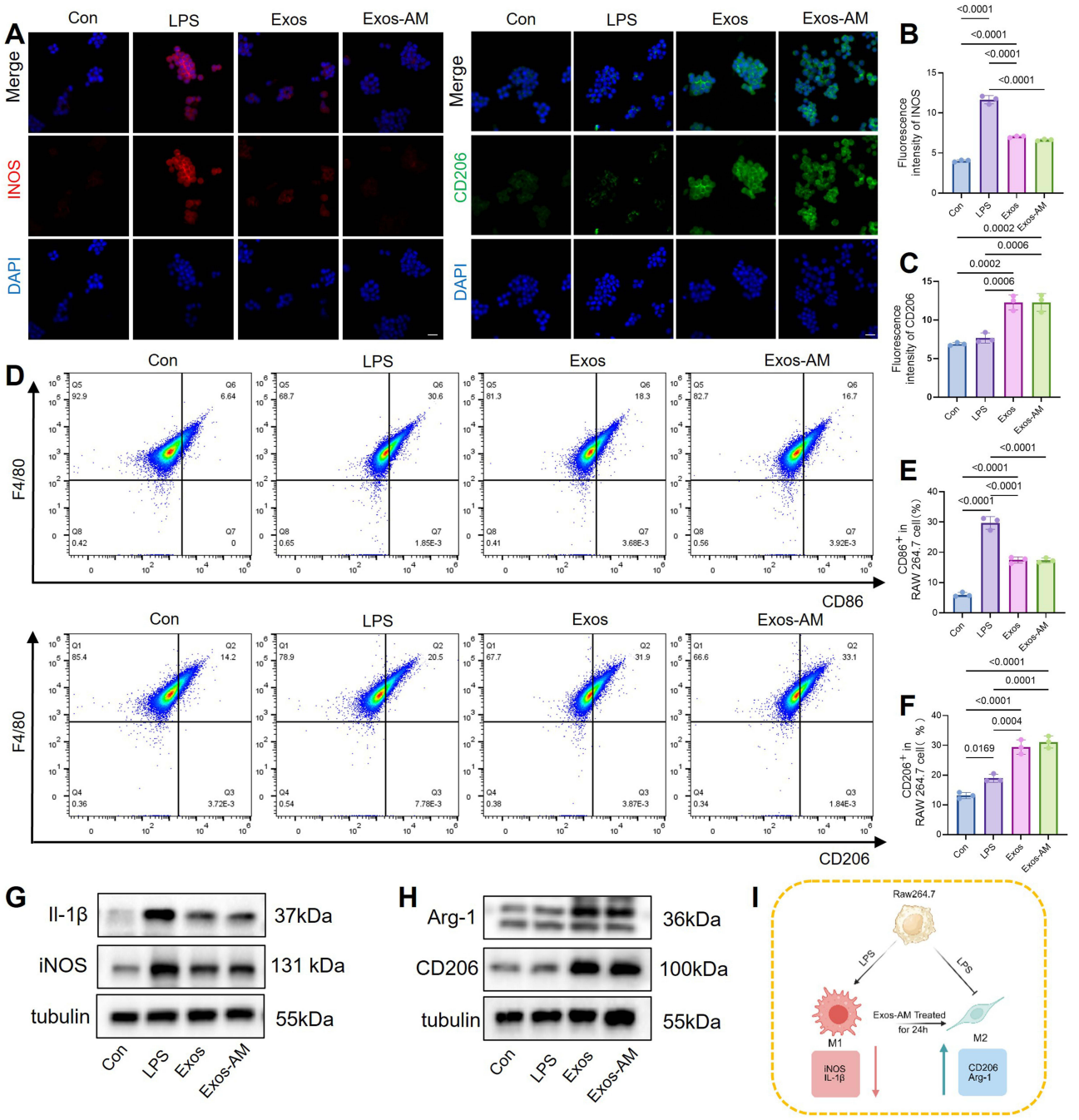

Figure 5 Exos-AM modulates macrophage polarization from M1 to M2 phenotype. (**A**) Immunofluorescence staining of iNOS and CD206 in RAW264.7. Bar = 10 μm. (**B** and **C**) Quantification of fluorescence intensity of iNOS (**B**) and CD206 (**C**) in RAW264.7. (**D**) Flow cytometry analysis of F4/80^{+}CD86^{+} and F4/80^{+}CD206^{+}. (**E** and **F**) Statistical analysis of the proportion of CD86^{+} (**E**) and CD206^{+} (**G**) Western blot analysis of IL-1β and iNOS. (**H**) Western blot analysis of Arg-1 and CD206. Data are presented as mean ± SD. (**I**) Schematic illustration of macrophage polarization, upward arrows indicate upregulation, and downward arrows indicate downregulation. Data are presented as mean ± SD.

promote M2-like polarization independently of drug loading.[60,61] This intrinsic activity of the exosome appears to be a key contributor to the observed anti-inflammatory effects. While ampicillin loading enhances antibacterial efficacy, the modulation of macrophage polarization is primarily driven by the exosomal components, which likely facilitate immune modulation and tissue repair through the M2 polarization pathway.

https://doi.org/10.2147/IJN.S578352

Exos and Exos-AM Suppress TGF-β1-Induced Fibrotic Activation in L929 Fibroblasts

To assess the effects of Exos and Exos-AM on fibrotic activation, L929 fibroblasts were treated with TGF-β1 (5 ng/mL) to induce a fibrotic phenotype,[62] followed by treatment with either Exos or Exos-AM. Both treatments significantly attenuated TGF-β1-induced fibroblast activation, as demonstrated by the results of the Transwell migration assay and scratch wound healing assay.

In the Transwell migration assay (Figure 6A), both Exos and Exos-AM treatments resulted in a significant reduction in the number of migrating fibroblasts compared with the TGF-β1-treated control group. The cell migration rate in both treatment groups was similarly decreased by approximately 40% relative to the TGF-β1 group (Figure 6B), indicating that both Exos and Exos-AM effectively inhibit fibroblast migration, which is a crucial step in fibrosis progression.

Similarly, in the scratch wound healing assay (Figure 6C), the migration of L929 cells into the wound area was significantly reduced in both Exos and Exos-AM treatment groups. The closure rate of the wound was substantially

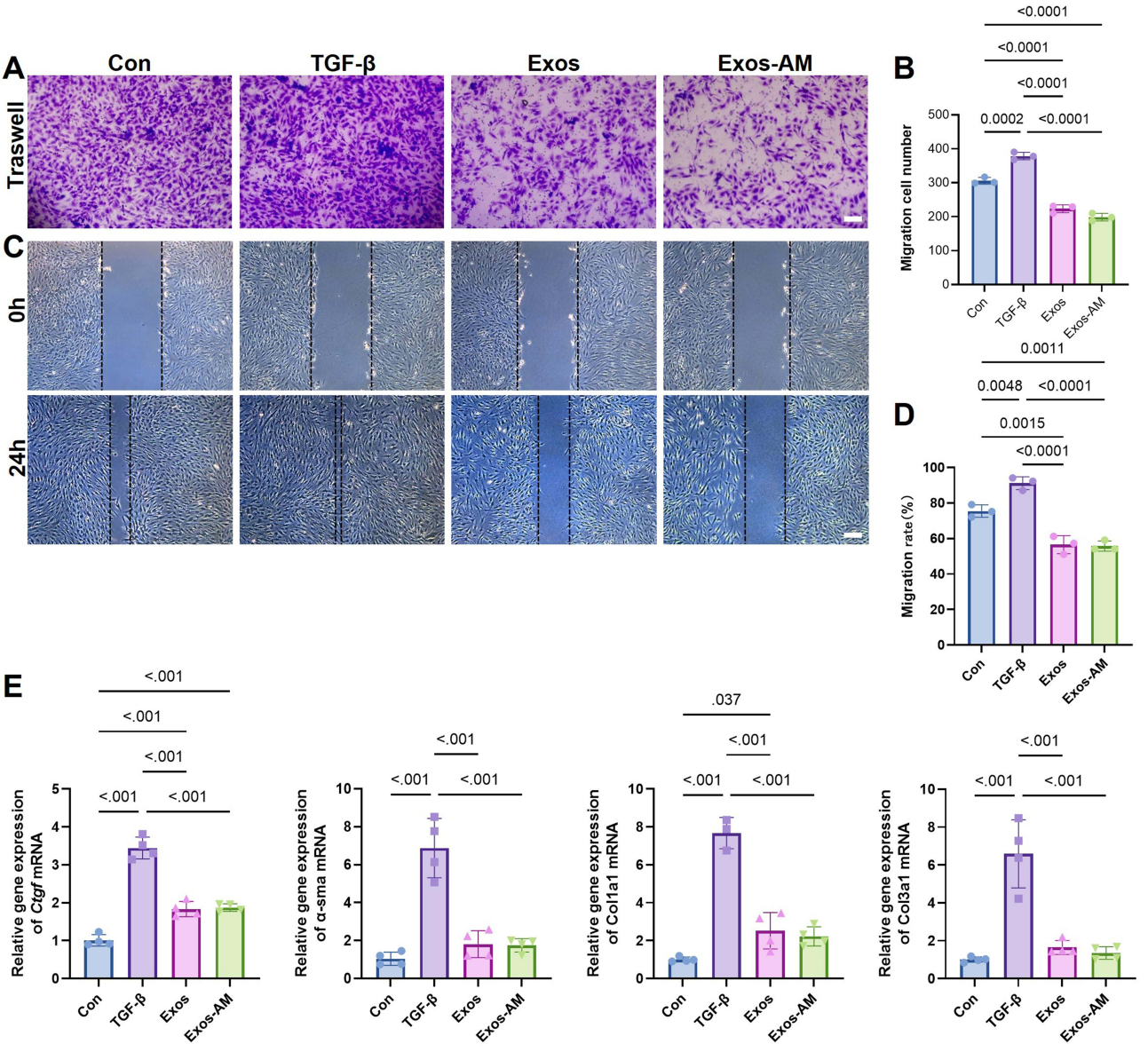

Figure 6 Effects of Exos and Exos-AM on L929 fibrotic activation. (**A**) Transwell migration assay of L929. Bar = 100μm. (**B**) Quantification of the number of migrating cells in the Transwell assay. (**C**) Scratch wound healing assay images at 0h and 24h. Bar = 100μm (**D**) Quantification of the number of migrating cells in the scratch wound healing assay. (**E**) Relative mRNA expression levels of *Ctgf, α-sma, Col1a1* and *Col3a1* in L929. Data are presented as mean ± SD.

https://doi.org/10.2147/IJN.S578352

slower in the treated groups compared to the TGF-β1 group (Figure 6D), further supporting the notion that both treatments can inhibit fibroblast migration and wound closure.

At the molecular level, RT-qPCR analysis (Figure 6E) showed that both Exos and Exos-AM treatments significantly reduced the expression of fibrosis-associated genes, including *α-SMA, Col1a1, Col3a1*, and *Ctgf*,[63] compared with the TGF-β1 group. The relative expression levels of these genes in the Exos and Exos-AM groups were similar, indicating that both formulations exert comparable effects in modulating the fibrotic response at the gene expression level.

These results suggest that both Exos and Exos-AM effectively suppress TGF-β1-induced fibrotic activation in L929 fibroblasts through mechanisms that likely involve the modulation of key fibrotic markers and the inhibition of fibroblast migration. Coincidentally, more studies on exosomes inhibiting fibrosis have been reported earlier.[64,65] Although the incorporation of ampicillin into Exos-AM may provide additional antibacterial benefits, the fibrotic suppression capabilities of Exos and Exos-AM are similar, which underscores the therapeutic potential of both formulations in mitigating fibrosis and tissue scarring.

Although Exos-AM and native Exos showed similar anti-inflammatory and anti-fibrotic effects, Exos-AM exhibited superior antibacterial activity. In COPD, bacterial infection often worsens inflammation and tissue injury, so loading ampicillin aimed to deliver antibiotics locally to infected lung tissues while reducing systemic side effects. Since ampicillin itself has no anti-inflammatory or anti-fibrotic action, the comparable results between Exos-AM and native Exos are expected. The main advantage of Exos-AM is its ability to enhance drug stability, increase local concentration, and add antibacterial function, offering strong potential for COPD treatment.

Transcriptomic Analysis Reveals the Mechanism of Exos-AM in Regulating LPS-Stimulated RAW264.7 Macrophages

To further investigate the underlying molecular mechanisms by which Exos-AM modulates LPS-induced macrophage activation, RNA sequencing was performed on RAW264.7 cells treated with LPS alone or LPS + Exos-AM. Person correlation analysis (Figure 7A) revealed a high correlation between the gene expression profiles of LPS + Exos-AM treated macrophages and LPS-treated controls. Differential gene expression analysis revealed a total of 966 upregulated genes and 967 downregulated genes in the Exos-AM group compared to the LPS group (Figure 7B), suggesting that Exos-AM treatment significantly alters the transcriptional profile of LPS-stimulated macrophages.

The volcano plot (Figure 7C) further highlighted the differentially expressed genes, with 1816 genes showing significant changes in expression (p-value < 0.05). Among these, 1313 genes were downregulated, and 503 genes were upregulated, indicating a broad modulation of macrophage response by Exos-AM.

Cluster analysis through a heatmap (Figure 7D) displayed clear separation between the LPS and LPS + Exos-AM groups, confirming the significant transcriptomic changes induced by Exos-AM. This suggests that Exos-AM not only mitigates the LPS-induced inflammatory response but also regulates the overall gene expression pattern associated with immune modulation.

To identify the pathways involved, we conducted KEGG enrichment analysis (Figure 7E), which revealed several enriched signaling pathways related to inflammation and immune responses. Notably, pathways such as TNF signaling, MAPK signaling, and NF-kB signaling were significantly enriched, suggesting that Exos-AM influences these critical pathways involved in macrophage activation and inflammatory responses. The TNF signaling pathway (Figure 7F) showed a strong enrichment score (ES = 0.23), indicating that Exos-AM treatment inhibits TNF-related inflammatory signaling. Similarly, the MAPK signaling pathway (Figure 7G) and the NF-kB signaling pathway (Figure 7H) were also negatively regulated by Exos-AM, further supporting the notion that Exos-AM suppresses the pro-inflammatory pathways activated by LPS.

To validate the transcriptomic findings, RT-qPCR was performed for representative genes associated with NF-κB and MAPK signaling pathways, including *Nfkb1, Mapk14*, and *Tnf*. The RT-qPCR results confirmed significant downregulation of these genes in Exos-AM–treated macrophages compared with the LPS group, consistent with the transcriptomic analysis (Supplementary Figure S2). These results further support that Exos-AM suppresses inflammatory signaling through coordinated inhibition of NF-κB and MAPK activation.

https://doi.org/10.2147/IJN.S578352

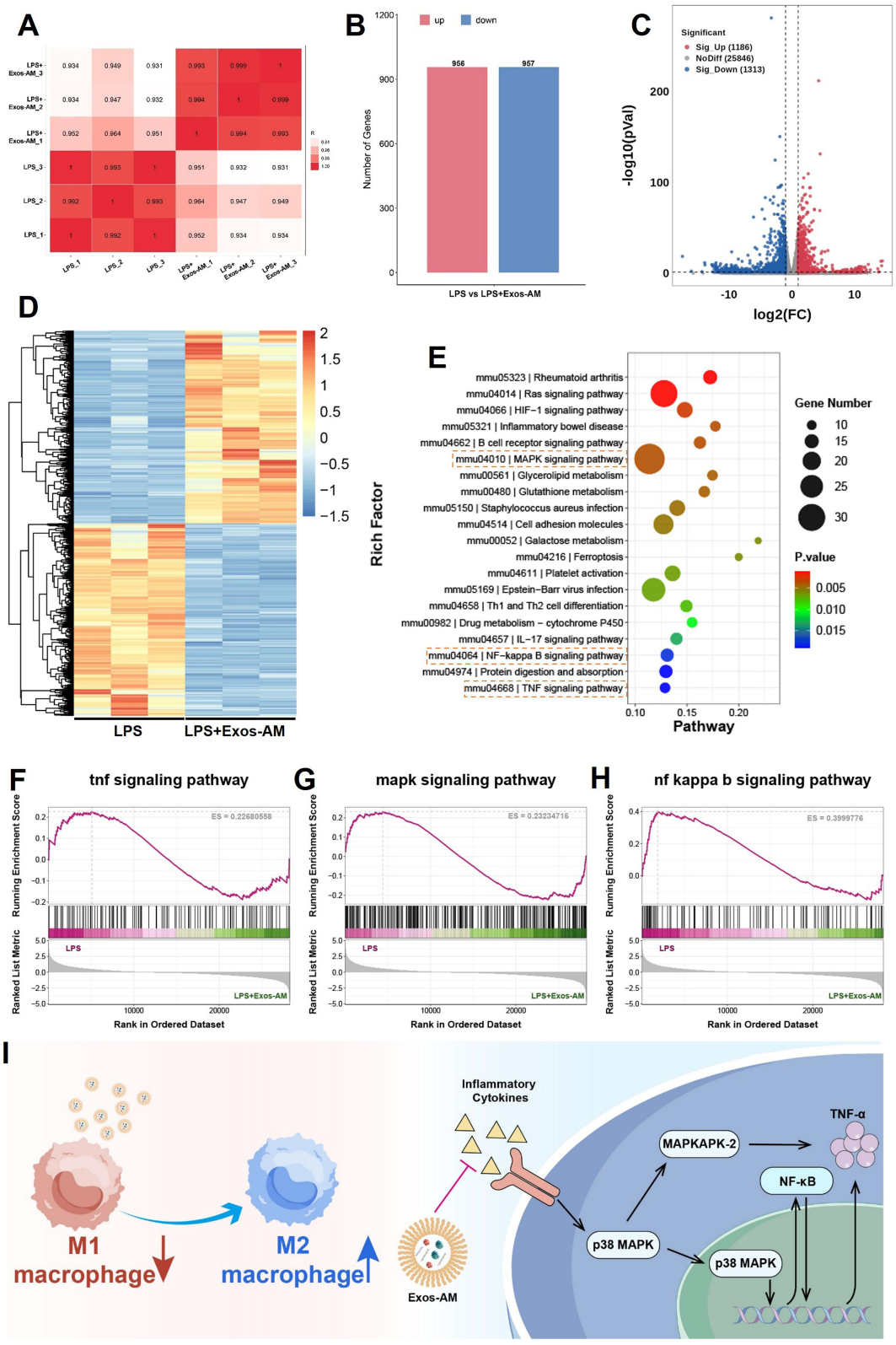

Figure 7 Transcriptomic analysis of RAW264.7. (**A**) Pearson's correlation coefficient. (**B**) The number of upregulated and downregulated genes. (**C**) Volcano plot. (**D**) Hierarchical clustering heatmap. (**E**) KEGG enrichment scatter plot. (**F**–**H**) GSEA plots showing the enrichment scores (ES) for the TNF signaling pathway (**F**) MAPK signaling pathway (**G**) and NF-kappa B signaling pathway (**H**). (**I**) Schematic diagram showing the modulation of macrophage polarization by Exos-AM. Upward arrows indicate upregulation, and downward arrows indicate downregulation.

These findings provide valuable insights into the molecular mechanisms underlying the immunomodulatory effects of Exos-AM. The downregulation of key pro-inflammatory pathways, such as TNF, MAPK, and NF-kB, suggests that Exos-AM exerts its anti-inflammatory effects through the attenuation of these well-established inflammatory signaling cascades (Figure 7I).[66–68] The ability of Exos-AM to modulate these pathways may explain its efficient repolarization of macrophages from the pro-inflammatory M1 phenotype towards the anti-inflammatory M2 phenotype, as observed in the previous sections. However, as no pathway-specific inhibitors or activators were employed, this evidence reflects a correlative relationship rather than a confirmed causal mechanism.

Therapeutic Effect of Exos-AM in a Mouse COPD Model

To evaluate the therapeutic potential of Exos-AM in a murine model of chronic obstructive pulmonary disease (COPD), mice were exposed to a combination of LPS and cigarette smoke, followed by *P. aeruginosa* infection and treatment with Exos or Exos-AM. The experimental timeline and treatment regimen are depicted in Figure 8A. Upon examination of lung tissue by H&E staining (Figure 8B), the COPD model exhibited severe pulmonary damage, characterized by the destruction of alveolar structures and extensive inflammatory infiltration. Treatment with Exos and Exos-AM resulted in partial restoration of lung structure, with Exos-AM treatment showing the most prominent improvement in alveolar integrity.

Immunofluorescence staining for CD206 and CD86 in lung sections (Figure 8C) further demonstrated that both Exos and Exos-AM treatments promoted M2 polarization. The Exos-AM group exhibited the highest number of CD206-positive cells, suggesting enhanced anti-inflammatory macrophage polarization in comparison to the Exos and control groups. The CD86-positive cells were significantly reduced in the Exos-AM group, highlighting the shift from the M1 to M2 phenotype, which is beneficial for the resolution of inflammation.

The bactericidal effects of Exos and Exos-AM were also evaluated in this COPD model by assessing the survival of *P. aeruginosa* in the lung tissue. As shown in Figure 8D and E, the colony count of *P. aeruginosa* was significantly reduced in the Exos and Exos-AM treatment groups, with Exos-AM showing the greatest reduction in bacterial survival, nearly achieving a complete bacterial clearance. This indicates that Exos-AM not only promotes macrophage polarization but also enhances bacterial clearance, contributing to the attenuation of infection in the COPD model. These findings indicate that Exos-AM primarily promotes early therapeutic responses: inflammation resolution and partial tissue repair.

However, one limitation of this study is the relatively short 3-week exposure period, which may not fully reproduce the chronic fibrotic changes observed in long-term COPD models. Future studies will explore extended exposure durations to better characterize progressive airway remodeling. Another limitation of this study is the lack of in vivo data on the pharmacokinetics, biodistribution, and release kinetics of ampicillin after Exos-AM nebulization. Moreover, chronic structural changes and lung function were not assessed due to experimental constraints. Future studies will address these aspects to better evaluate the long-term efficacy and translational potential of Exos-AM.

From a translational perspective, although plant-derived exosomes exhibit excellent biocompatibility and therapeutic potential, their large-scale application remains challenging due to limitations in yield, purification efficiency, and compositional consistency. Future studies should focus on improving scalability and standardization to ensure reproducibility and clinical feasibility. Together, these findings demonstrate that Exos-AM treatment significantly attenuates COPD progression and inflammation in a murine model. The combined effects of promoting M2 macrophage polarization and enhancing bacterial clearance underscore the therapeutic potential of Exos-AM in treating chronic inflammatory lung diseases, such as COPD.

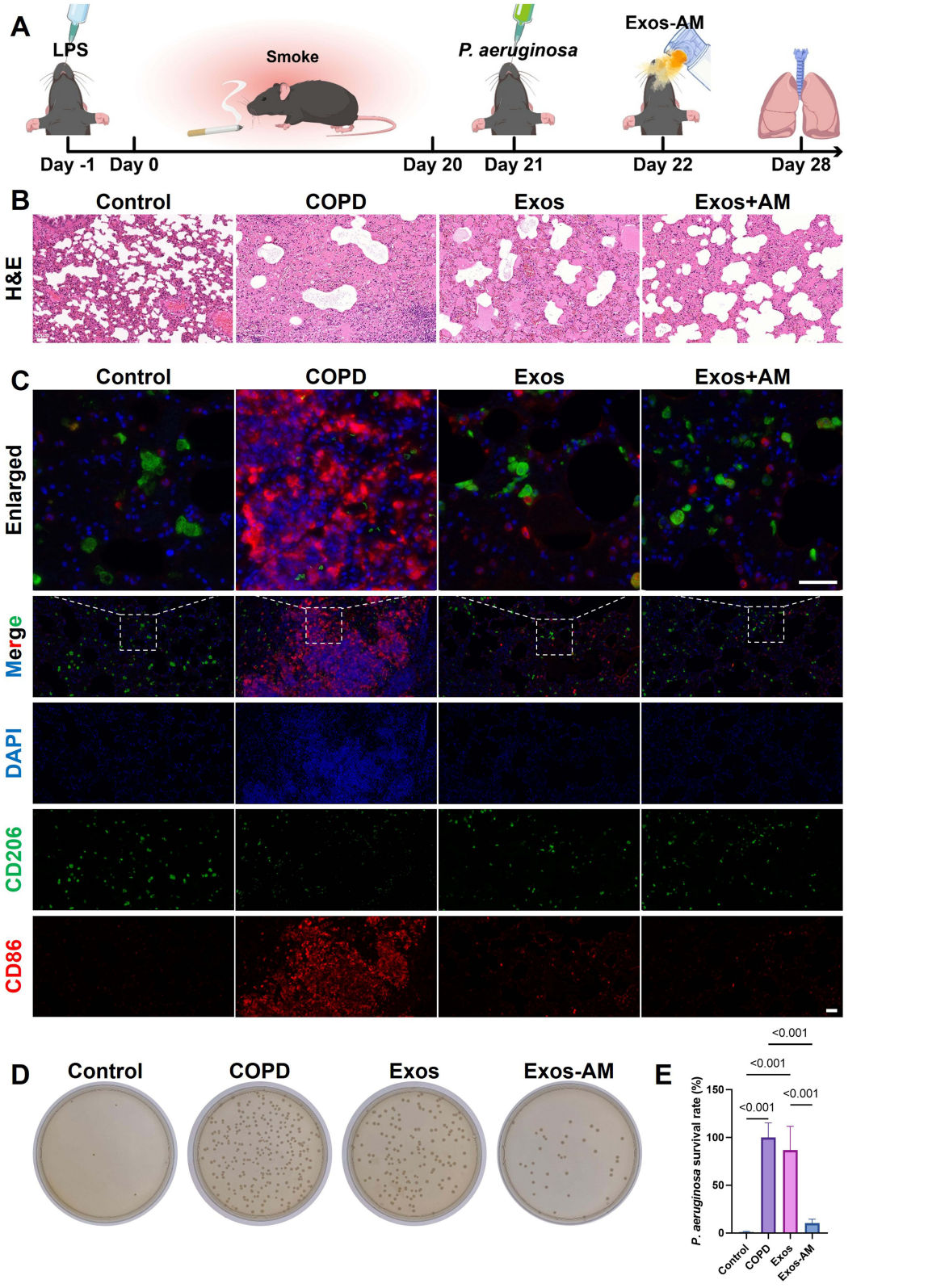

Figure 8 Therapeutic effect of Exos-AM in a mouse COPD model. (**A**) Experimental timeline showing the procedure. (**B**) H&E staining of lung tissue sections. Bar = 50μm (**C**) Immunofluorescence images of lung tissue showing CD86 and CD206. (**D**) Colony formation assay of *P. aeruginosa* Bar = 50 μm. (**E**) Quantification of *P. aeruginosa* survival rate. Data are presented as mean ± SD.

https://doi.org/10.2147/IJN.S578352

Conclusion

In this study, we successfully developed ampicillin-loaded fenugreek-derived exosomes (Exos-AM) as a plant-based therapeutic platform for managing Chronic Obstructive Pulmonary Disease (COPD). Our results demonstrate that Exos-AM exhibits strong antioxidant, anti-inflammatory, and antibacterial activities, thereby addressing key pathogenic factors of COPD. The encapsulation of ampicillin into fenugreek exosomes enhanced antibacterial efficacy against common pulmonary pathogens such as *Staphylococcus aureus, Escherichia coli*, and *Pseudomonas aeruginosa*, while the exosomal matrix itself promoted macrophage polarization toward the anti-inflammatory M2 phenotype. This macrophage modulation contributed to reduced airway inflammation, limited fibrotic remodeling, and mitigation of COPD progression.

Moreover, Exos-AM showed excellent biocompatibility both in vitro and in vivo, with no evident adverse effects on major organs. These findings highlight the potential of fenugreek-derived exosomes as a versatile and biocompatible drug delivery platform. While ampicillin loading reinforces antibacterial performance, the anti-inflammatory and tissue-protective effects largely stem from the intrinsic properties of the exosomes. In conclusion, this work establishes Exos-AM as a promising foundation for exosome-based therapy in COPD, offering complementary antimicrobial and immunomodulatory benefits. Future studies should optimize formulation parameters, assess long-term safety, and explore clinical translation to realize its therapeutic potential.

Data Sharing Statement

Data available on request from the corresponding author.

Ethical Statement

The animal experiment in this study was approved by the Institutional Animal Care and Use Committee (IACUC) of the Respiratory Center, GUANGZHOU Seyotin BIO-TECH CO.Ltd (Approval No. SYT2024155). All experimental procedures involving animals were conducted in strict accordance with the *Guidelines for the Ethical Review of Laboratory Animal Welfare (GB/T 35892–2018)*.

Funding

This study was supported by Natural Science Foundation of Xinjiang Uygur Autonomous Region (No. 2023D03018); Tianshan Talents Medical and Health High Level Talent Project (No. TSYC202401B111).

Disclosure

The authors report no conflicts of interests in this work.

References

1. Alvar A, Dave S, Rosa FJNRDD. Treatment of chronic obstructive pulmonary disease: current pipeline and new opportunities. 2025.
2. Francesca P, Don DSJARP. The developmental origins of asthma and COPD. 2025.
3. Bennitt FB, Wozniak S, Causey K, et al. Global, regional, and national burden of household air pollution, 1990-2021: a systematic analysis for the Global Burden of Disease Study 2021. *J Lancet*. 2025;405(10485).
4. D'Arcy ME, Pfeiffer RM, Bradley MC, et al. Inflammatory diseases and risk of lung cancer among individuals who have never smoked. *Nat Commun*. 2025;16(1).
5. Budden KF, Shukla SD, Bowerman KL, et al. Faecal microbial transfer and complex carbohydrates mediate protection against COPD. *Gut*. 2024;73(5).
6. Brake SJ, Lu W, Chia C, et al. Transforming growth factor-β1 and SMAD signalling pathway in the small airways of smokers and patients with COPD: potential role in driving fibrotic type-2 epithelial mesenchymal transition. *Front Immunol*. 2023;14:1216506. doi:10.3389/fimmu.2023.1216506
7. Baßler K, Fujii W, Kapellos TS, et al. Alveolar macrophages in early stage COPD show functional deviations with properties of impaired immune activation. *Front Immunol*. 2022;13:917232. doi:10.3389/fimmu.2022.917232
8. Barnes PJ. Cellular and molecular mechanisms of asthma and COPD. *Clin Sci*. 2017;131(13):1541–1558. doi:10.1042/CS20160487
9. Booth S, Hsieh A, Mostaco-Guidolin L, et al. A Single-Cell atlas of small airway disease in chronic obstructive pulmonary disease: a cross-sectional study. *Am J Respir Crit Care Med*. 2023;208(4).
10. Alanazi FJ, Alruwaili AN, Aldhafeeri NA, et al. Pathological interplay of NF-κB and M1 macrophages in chronic inflammatory lung diseases. *Pathol Res Pract*. 2025;269:155903. doi:10.1016/j.prp.2025.155903
11. Guo B, Shi X, Jiang Q, et al. Targeting immunoproteasome in polarized macrophages ameliorates experimental emphysema via activating NRF1/2-P62 axis and suppressing IRF4 transcription. *Advanc Sci*. 2024;11(44).

12. Ji Y, Li X, Yao X, et al. Macrophage polarization: molecular mechanisms, disease implications, and targeted therapeutic strategies. *Front Immunol*. 2025;16:1732718. doi:10.3389/fimmu.2025.1732718
13. Rodríguez-Pérez J, Andreu-Martínez R, Daza R, et al. Oxidative stress and inflammation in hypoxemic respiratory diseases and their comorbidities: molecular insights and diagnostic advances in chronic obstructive pulmonary disease and sleep apnea. *Antioxidants*. 2025;14(7).
14. Cabrera-Fuentes HA, Lopez ML, McCurdy S, et al. Regulation of monocyte/macrophage polarisation by extracellular RNA. *Thrombosis Haemostasis*. 2015;113(3):473–481. doi:10.1160/TH14-06-0507
15. Neu C, Thiele Y, Horr F, et al. DAMPs released from proinflammatory macrophages induce inflammation in cardiomyocytes via activation of TLR4 and TNFR. *Int J Mol Sci*. 2022;23(24):15522. doi:10.3390/ijms232415522
16. Ramalingam PS, Afzal M, Babu MA, et al. Targeting cancer via macrophage-derived exosomal miRNAs: implications for tumor progression and resistance. *Front Immunol*. 2025;16:1683799. doi:10.3389/fimmu.2025.1683799
17. Wedzicha JA, Seemungal TA. COPD exacerbations: defining their cause and prevention. *Lancet*. 2007;370(9589):786–796. doi:10.1016/S0140-6736(07)61382-8
18. Martinez-Garcia MA, Miravitlles M. The impact of chronic bronchial infection in COPD: a proposal for management. *Int J Chronic Obstr*. 2022;17:621–630. doi:10.2147/COPD.S357491
19. Qin S, Xiao W, Zhou C, et al. P*seudomonas aeruginosa*: pathogenesis, virulence factors, antibiotic resistance, interaction with host, technology advances and emerging therapeutics. *Signal Transduct Target Ther*. 2022;7(1):199. doi:10.1038/s41392-022-01056-1
20. Elbehairy AF, Marshall H, Naish JH, et al. Advances in COPD imaging using CT and MRI: linkage with lung physiology and clinical outcomes. *Europ Resp J*. 2024;63(5):2301010. doi:10.1183/13993003.01010-2023
21. Rao W, Wang S, Duleba M, et al. Regenerative metaplastic clones in COPD lung drive inflammation and fibrosis. *Cell*. 2020;181(4):848–864.e818. doi:10.1016/j.cell.2020.03.047
22. Barnes PJ. Small airway fibrosis in COPD. *Int J Biochem Cell Biol*. 2019;116:105598. doi:10.1016/j.biocel.2019.105598
23. Zhang M, Wang W, Liu K, Jia C, Hou Y, Bai G. Astragaloside IV protects against lung injury and pulmonary fibrosis in COPD by targeting GTP-GDP domain of RAS and downregulating the RAS/RAF/FoxO signaling pathway. *Phytomedicine*. 2023;120:155066. doi:10.1016/j.phymed.2023.155066
24. Labaki WW, Rosenberg SR. Chronic obstructive pulmonary disease. *Ann Internal Med*. 2020;173(3):Itc17–itc32. doi:10.7326/AITC202008040
25. MacLeod M, Papi A, Contoli M, et al. Chronic obstructive pulmonary disease exacerbation fundamentals: diagnosis, treatment, prevention and disease impact. *Respirology*. 2021;26(6):532–551. doi:10.1111/resp.14041
26. Pegtel DM, Gould SJ. Exosomes. *Annu Rev Biochem*. 2019;88:487–514. doi:10.1146/annurev-biochem-013118-111902
27. Kalluri R, LeBleu VS. The biology, function, and biomedical applications of exosomes. *Science*. 2020;367(6478). doi:10.1126/science.aau6977
28. Yan W, Jiang S. Immune Cell-Derived exosomes in the Cancer-Immunity cycle. *Trends Cancer*. 2020;6(6):506–517. doi:10.1016/j.trecan.2020.02.013
29. Song Y, You Y, Xu X, et al. Adipose-Derived mesenchymal stem cell-derived exosomes biopotentiated extracellular matrix hydrogels accelerate diabetic wound healing and skin regeneration. *Adv Sci*. 2023;10(30):e2304023. doi:10.1002/advs.202304023
30. Zhang S, Teo KYW, Chuah SJ, Lai RC, Lim SK, Toh WS. MSC exosomes alleviate temporomandibular joint osteoarthritis by attenuating inflammation and restoring matrix homeostasis. *Biomaterials*. 2019;200:35–47. doi:10.1016/j.biomaterials.2019.02.006
31. Kim J, Zhu Y, Chen S, et al. Anti-glioma effect of ginseng-derived exosomes-like nanoparticles by active blood-brain-barrier penetration and tumor microenvironment modulation. *J Nanobiotechnol*. 2023;21(1):253. doi:10.1186/s12951-023-02006-x
32. Teng Y, Xu F, Zhang X, et al. Plant-derived exosomal microRNAs inhibit lung inflammation induced by exosomes SARS-CoV-2 Nsp12. *Mol Ther*. 2021;29(8):2424–2440. doi:10.1016/j.ymthe.2021.05.005
33. Kim J, Li S, Zhang S, Wang J. Plant-derived exosome-like nanoparticles and their therapeutic activities. *Asian J Pharm Sci*. 2022;17(1):53–69. doi:10.1016/j.ajps.2021.05.006
34. Zhao B, Lin H, Jiang X, et al. Exosome-like nanoparticles derived from fruits, vegetables, and herbs: innovative strategies of therapeutic and drug delivery. *Theranostics*. 2024;14(12):4598–4621. doi:10.7150/thno.97096
35. Jadoon S, Karim S, Bin Asad MH, et al. Anti-Aging potential of phytoextract loaded-pharmaceutical creams for human skin cell longetivity. *Oxid Med Cell Longev*. 2015;2015:709628. doi:10.1155/2015/709628
36. Nagulapalli Venkata KC, Swaroop A, Bagchi D, Bishayee A. A small plant with big benefits: fenugreek (Trigonella foenum-graecum Linn.) for disease prevention and health promotion. *Mol Nutr Food Res*. 2017;61(6). doi:10.1002/mnfr.201600950
37. Li M, Huang H, Wei X, et al. Clinical investigation on nebulized human umbilical cord MSC-derived extracellular vesicles for pulmonary fibrosis treatment. *Signal Transduct Target Ther*. 2025;10(1):179. doi:10.1038/s41392-025-02262-3
38. Zhu YG, Shi MM, Monsel A, et al. Nebulized exosomes derived from allogenic adipose tissue mesenchymal stromal cells in patients with severe COVID-19: a pilot study. *Stem Cell Res Ther*. 2022;13(1):220. doi:10.1186/s13287-022-02900-5
39. Herath SC, Normansell R, Maisey S, Poole P. Prophylactic antibiotic therapy for chronic obstructive pulmonary disease (COPD). *Cochrane Database Syst Rev*. 2018;10(10):Cd009764. doi:10.1002/14651858.CD009764.pub3
40. Yu Q, Zhang Q, Zhu J, et al. Inhalable neutrophil-mimicking nanoparticles for chronic obstructive pulmonary disease treatment. *J Control Release*. 2025;381:113648. doi:10.1016/j.jconrel.2025.113648
41. Krylova SV, Feng D. The machinery of exosomes: biogenesis, release, and uptake. *Int J Mol Sci*. 2023;24(2):1337. doi:10.3390/ijms24021337
42. Liang Y, Duan L, Lu J, Xia J. Engineering exosomes for targeted drug delivery. *Theranostics*. 2021;11(7):3183–3195. doi:10.7150/thno.52570
43. Lai JJ, Chau ZL, Chen SY, et al. Exosome processing and characterization approaches for research and technology development. *Adv Sci*. 2022;9(15):e2103222. doi:10.1002/advs.202103222
44. Bai C, Liu J, Zhang X, et al. Research status and challenges of plant-derived exosome-like nanoparticles. *Biomed Pharmacothe*. 2024;174:116543. doi:10.1016/j.biopha.2024.116543
45. Sha A, Luo Y, Xiao W, et al. Plant-Derived exosome-like nanoparticles: a comprehensive overview of their composition, biogenesis, isolation, and biological applications. *Int J Mol Sci*. 2024;25(22):12092. doi:10.3390/ijms252212092
46. Pandey H, Awasthi P. Effect of processing techniques on nutritional composition and antioxidant activity of fenugreek (Trigonella foenum-graecum) seed flour. *J Food Sci Technol*. 2015;52(2):1054–1060. doi:10.1007/s13197-013-1057-0
47. Luo W, Deng J, He J, et al. Integration of molecular docking, molecular dynamics and network pharmacology to explore the multi-target pharmacology of fenugreek against diabetes. *J Cell Mol Med*. 2023;27(14):1959–1974. doi:10.1111/jcmm.17787

48. Zameer S, Najmi AK, Vohora D, Akhtar M. A review on therapeutic potentials of Trigonella foenum graecum (fenugreek) and its chemical constituents in neurological disorders: complementary roles to its hypolipidemic, hypoglycemic, and antioxidant potential. *Nutr Neurosci*. 2018;21(8):539–545. doi:10.1080/1028415X.2017.1327200
49. Selvaraj S, Fathima NN. Fenugreek incorporated silk fibroin nanofibers-a potential antioxidant scaffold for enhanced wound healing. *ACS Appl Mater Interfaces*. 2017;9(7):5916–5926. doi:10.1021/acsami.6b16306
50. Yang X, Shi G, Guo J, Wang C, He Y. Exosome-encapsulated antibiotic against intracellular infections of methicillin-resistant *Staphylococcus aureus*. *Int J Nanomed*. 2018;13:8095–8104. doi:10.2147/IJN.S179380
51. Cooke AC, Nello AV, Ernst RK, Schertzer JW. Analysis of *Pseudomonas aeruginosa* biofilm membrane vesicles supports multiple mechanisms of biogenesis. *PLoS One*. 2019;14(2):e0212275. doi:10.1371/journal.pone.0212275
52. Vasilyeva NV, Tsfasman IM, Suzina NE, Stepnaya OA, Kulaev IS. Secretion of bacteriolytic endopeptidase L5 of lysobacter sp. XL1 into the medium by means of outer membrane vesicles. *FEBS J*. 2008;275(15):3827–3835. doi:10.1111/j.1742-4658.2008.06530.x
53. Lima LM, Silva B, Barbosa G, Barreiro EJ. β-lactam antibiotics: an overview from a medicinal chemistry perspective. *Eur J Med Chem*. 2020;208:112829. doi:10.1016/j.ejmech.2020.112829
54. Wang X, Zhou H, Li D, et al. Molecular targeting of intracellular bacteria by homotypic recognizing nanovesicles for infected pneumonia treatment. *Biomater Res*. 2025;29:0172. doi:10.34133/bmr.0172
55. Zou J, Cui W, Deng N, et al. Fate reversal: exosome-driven macrophage rejuvenation and bacterial-responsive drug release for infection immunotherapy in diabetes. *J Control Release*. 2025;382:113730. doi:10.1016/j.jconrel.2025.113730
56. Tian Y, Li S, Song J, et al. A doxorubicin delivery platform using engineered natural membrane vesicle exosomes for targeted tumor therapy. *Biomaterials*. 2014;35(7):2383–2390. doi:10.1016/j.biomaterials.2013.11.083
57. Zhuo Y, Luo Z, Zhu Z, et al. Direct cytosolic delivery of siRNA via cell membrane fusion using cholesterol-enriched exosomes. *Nature Nanotechnol*. 2024;19(12):1858–1868. doi:10.1038/s41565-024-01785-0
58. Wu Z, Cai YS, Yuan R, et al. Bioactive pterocarpans from Trigonella foenum-graecum L. *Food Chem*. 2020;313:126092. doi:10.1016/j.foodchem.2019.126092
59. Chi L, Niu H, Niu Y, et al. Trigonella foenum-graecum L. ameliorates metabolism-associated fatty liver disease in type 2 diabetic mice: a multi-omics mechanism analysis. *J Ethnopharmacol*. 2025;348:119862. doi:10.1016/j.jep.2025.119862
60. Zhuang X, Deng ZB, Mu J, et al. Ginger-derived nanoparticles protect against alcohol-induced liver damage. *J Extracell Vesicles*. 2015;4:28713. doi:10.3402/jev.v4.28713
61. Kim Y, Kim YK, Lee S, Kim M, Lee SW, Lee YH. Panax ginseng-derived Exosome-like nanoparticles prevent LPS-induced septic shock by modulating TLR4 glycosylation in macrophages. *Mol Pharmaceut*. 2026. doi:10.1021/acs.molpharmaceut.5c00113
62. Zhang J, Chen X, Chen H, et al. Engeletin ameliorates pulmonary fibrosis through endoplasmic reticulum stress depending on lnc949-mediated TGF-β1-Smad2/3 and JNK signalling pathways. *Pharm Biol*. 2020;58(1):1105–1114. doi:10.1080/13880209.2020.1834590
63. Um IG, Woo JS, Lee YJ, et al. IL-21 drives skin and lung inflammation and fibrosis in a model for systemic sclerosis. *Immunol Lett*. 2024;270:106924. doi:10.1016/j.imlet.2024.106924
64. Lin Y, Li Y, Chen P, et al. Exosome-Based regimen rescues endometrial fibrosis in intrauterine adhesions via targeting clinical fibrosis biomarkers. *Stem Cells Translat Med*. 2023;12(3):154–168. doi:10.1093/stcltm/szad007
65. Yang Y, Zhang J, Wu S, et al. Exosome/antimicrobial peptide laden hydrogel wound dressings promote scarless wound healing through miR-21-5p-mediated multiple functions. *Biomaterials*. 2024;308:122558. doi:10.1016/j.biomaterials.2024.122558
66. Huang Y, Li G, Li D, et al. Ethyl caffeate alleviates inflammatory response and promotes recovery in septic-acute lung injury via the TNF-α/NF-κB/MMP9 Axis. *Phytomedicine*. 2025;141:156700. doi:10.1016/j.phymed.2025.156700
67. Liu L, Guo H, Song A, et al. Progranulin inhibits LPS-induced macrophage M1 polarization via NF-κB and MAPK pathways. *BMC Immunology*. 2020;21(1):32. doi:10.1186/s12865-020-00355-y
68. Mao N, Yu Y, Lu X, Yang Y, Liu Z, Wang D. Preventive effects of matrine on LPS-induced inflammation in RAW 264.7 cells and intestinal damage in mice through the TLR4/NF-κB/MAPK pathway. *Int Immunopharmacol*. 2024;143(Pt 2):113432. doi:10.1016/j.intimp.2024.113432